Delayed onset of inherited ALS by deletion of the BDNF receptor TrkB.T1 is non-cell autonomous

Sudhirkumar Yanpallewar,

Gianluca Fulgenzi,

Francesco Tomassoni-Ardori,

Colleen Barrick,

Lino Tessarollo[*]

Neural Development Section, Mouse Cancer Genetics Program, CCR, NCI, NIH, USA

Abstract

The pathophysiology of Amyotrophic Lateral Sclerosis (ALS), a disease caused by the gradual degeneration of motoneurons, is still largely unknown. Insufficient neurotrophic support has been cited as one of the causes of motoneuron cell death. Neurotrophic factors such as BDNF have been evaluated in ALS human clinical trials, but yielded disappointing results attributed to the poor pharmacokinetics and pharmacodynamics of BDNF. In the inherited ALS G93A SOD1 animal model, deletion of the BDNF receptor TrkB.T1 delays spinal cord motoneuron cell death and muscle weakness through an unknown cellular mechanism. Here we show that TrkB.T1 is expressed ubiquitously in the spinal cord and its deletion does not change the SOD1 mutant spinal cord inflammatory state suggesting that TrkB.T1 does not influence microglia or astrocyte activation. Although TrkB.T1 knockout in astrocytes preserves muscle strength and co-ordination at early stages of disease, its specific conditional deletion in motoneurons or astrocytes does not delay motoneuron cell death during the early stage of the disease. These data suggest that TrkB.T1 may limit the neuroprotective BDNF signaling to motoneurons via a non-cell autonomous mechanism providing new understanding into the reasons for past clinical failures and insights into the design of future clinical trials employing TrkB agonists in ALS.

Keywords

Receptor tyrosine kinase; Neurotrophin; BDNF; TrkB signaling; Truncated TrkB; Motoneuron degeneration; Spinal cord inflammation; ALS

1. Introduction

Amyotrophic lateral sclerosis (ALS) is a neurodegenerative disorder of the upper and lower motoneurons that currently has no effective treatment. Loss of these motoneurons leads to rapidly progressive and irreversible paralysis with swallowing and respiratory malfunctions

[*] Corresponding author at: NCI-Frederick, 7th Street, Bldg. 560, Frederick, MD 21702, USA. tessarol@mail.nih.gov (L. Tessarollo).

eventually resulting in death within 5 years of onset (Mitchell and Borasio 2007). Most ALS cases are sporadic, with only 5–10% of cases being inherited in an autosomal dominant fashion (Nguyen et al. 2018). Experimental evidence suggests that toxic misfolded protein aggregates, oxidative stress, glutamate excitotoxicity, lack of neurotrophic support and abnormal cell signaling leading to increased intracellular calcium are among the putative causes leading to the selective motoneuron loss and rapid progression of the disease (Boillee et al. 2006a). However, to date, no drug targeting these processes has been successful in providing a cure or ameliorating the disease outcome (Henriques et al. 2010; Katz et al. 2015).

Neurotrophic factors are potent modulators of neuronal survival and function. They influence proliferation, migration and differentiation of stem cells in the developing and adult nervous system and they regulate dendrite and synapse formation (Chao et al. 2006; Huang and Reichardt 2001; Kaplan and Miller 2000; Lu et al. 2013). The expression of neurotrophic factors in astrocytes, neurons, microglia and endothelial cells and their ability to induce neuronal regeneration in disease and injury models have suggested their use for the treatment of neurodegenerative diseases, including ALS (Buck et al. 2000; Gravel et al. 1997; Josephson et al. 2001; Tovar et al. 2014). Brain-derived Neurotrophic Factor (BDNF), the ligand for the TrkB tyrosine kinase receptor, was used in three separate clinical trials without efficacy most likely due to poor pharmacokinetics and pharmacodynamics (Beck et al. 2005; Group, 1999; Kalra et al. 2003; Ochs et al. 2000). A number of questions remain including whether or not BDNF has a sufficient half-life to generate long lasting effects and whether it reaches its target and activates its receptor/s to transduce survival signaling (Thoenen and Sendtner 2002). In addition, the lack of specific antibodies to study the cellular distribution of the different TrkB receptor isoforms in the spinal cord and how they influence BDNF function on diseased motoneurons have further hampered our understanding of the physiological and pathophysiological roles of BDNF in the spinal cord. At the biochemical level, it has been shown that the spinal cord dynamically expresses two major TrkB receptor isoforms during development (Zhang and Huang 2006) including: 1) a full length isoform with a tyrosine kinase domain (TrkB.Kin) activating the Ras/MAPK, phosphoinositide-3-kinase and phospholipase Cγ (PLCγ) pathways (Huang and Reichardt 2003; Tessarollo 1998); 2) a truncated TrkB.T1 isoform with dominant negative function but also with calcium release activity from the intracellular stores through a still unknown molecular mechanism (Carim-Todd et al. 2009; Dorsey et al. 2012; Fulgenzi et al. 2020; Fulgenzi et al. 2015; Rose et al. 2003). Expression levels of these isoforms are not affected by mutant SOD1 G93A (Zhang and Huang 2006). However, we have found that deletion of TrkB.T1 in the SOD1 G93A model delays lumbar spinal cord motoneuron cell death and muscle weakness (Yanpallewar et al. 2012). These data together with the observations that ALS patients have elevated BDNF and TrkB kinase levels but have a decrease in TrkB phosphorylation, suggest that the underlying pathology in ALS is not due to a lack of BDNF supply but a mechanism affecting the TrkB response to BNDF or an effect of BDNF on the development of spinal cord inflammatory processes (Kust et al. 2002; Mutoh et al. 2000). Thus, TrkB.T1 may limit BDNF diffusion to motoneurons or TrkB.T1 expressed in glia cells may elevate intracellular calcium levels which is part of the mechanism contributing to glia activation in pathological processes (Agulhon et al. 2008; Biffo et al. 1995; Kawamata

et al. 2014; Morse et al. 1993). Although TrkB is widely expressed in the mouse and human spinal cord, it is still unclear what the TrkB.T1 specific pattern of expression is due to a lack of specific antibodies. Therefore, we investigated TrkB.T1 distribution in the lumbar spinal cord using a TrkB.T1-tagged knock-in mouse model, followed by an analysis of TrkB.T1 deletion on the inflammatory state of mutant spinal cords and a cell-specific analysis of TrkB.T1 deletion on the SOD1 G93A-induced pathology to test TrkB.T1 cell-autonomous functions. We found that TrkB. T1 is expressed in all spinal cord cell populations, its knockout does not influence spinal cord reactive gliosis and conditional deletion in only motoneurons or astrocytes does not delay motoneuron cell death. However, astrocyte-specific deletion of TrkB.T1 partially improves motor performance and delays progression of the early phase of disease.

2.   Materials and methods

2.1.   Animals

TrkB.T1 knockout and TrkB.T1-V5 mice have been described previously (Dorsey et al. 2006; Fulgenzi et al. 2020). SOD1G93A [B6SJL-TG (SOD1*G93A)1GUR/J; 002726], GFAP-Cre [B6.Cg-Tg(GFAP-cre) 73.12Mvs/J; 012886] and HB9-Cre [B6.129S1-Mnx1tm4(cre)Tmj/J; 006600] transgenic mice were acquired from The Jackson Laboratory (Bar Harbor, ME). Mice were backcrossed on C57/B16J background for at least 10 generations before performing genetic experiments. SOD1-TrkB.T1 KO (SOD1 T) were described earlier (Quarta et al. 2018; Yanpallewar et al. 2012), whereas astrocyte-specific (GFAP cre-SOD1T1 CKO GFAP) or motor neuron-specific (HB9 cre- SOD1T1 CKO HB9) knockout of TrkB.T1 receptor in SOD1 G93A mutant mice were generated by crossing the conditional allele of TrkB.T1 (Dorsey et al. 2006) with the specific cre-Tg mouse and the SOD1 G93A allele. Conditional GFAP cre- SOD1T1 CKO and HB9 cre-SOD1T1 CKO mice were obtained by introducing a conditional (CKO) and a constitutive TrkB.T1 KO allele together with the cre transgene into the SOD1 mutant background to increase the efficiency of the cell-type specific recombination in astrocytes or motoneurons, respectively. This strategy greatly enhances the cell-type specific recombination since only one conditional allele has to undergo recombination. All procedures for mouse experiments were approved by the NCI-Frederick Animal Care and Use Committee (ACUC) and followed the National Institutes of Health Guidelines for animal care and use.

2.2.   Motor neuron survival and immunostaining

Twelve-week-old mice were anesthetized and perfused transcardially with 1xPBS followed by 4% paraformaldehyde. The lumbar spinal cord was isolated and 50-μm transverse sections were cut on a cryostat. Every 10th section (18–20 sections/animal) was collected for Nissl staining to analyze the number of surviving motor neurons (Yanpallewar et al. 2012). For immunostaining analysis, 5 sections/animal were first incubated with the primary antibody followed by the specific fluorescent conjugated secondary antibody. The following antibodies were used: Rabbit anti-GFAP (1:500, Dako), Rabbit anti-Iba1 (1:250, Wako), Rabbit anti-V5 mAb (1:200 Cell Signaling Technology), Rabbit anti-iNOS (1:500 BD Transduction Laboratories) and Rabbit anti-nitrotyrosine (1:500, Millipore). For comparison of GFAP and Iba1 immunoreactivities, immunofluorescence images were obtained under

constant setting on a confocal microscope and differences in florescent signal intensities between the genotypes were analyzed quantitatively using NIH Image J software.

2.3. Measurement of TNFα and IL-1β by ELISA

Lumbar spinal cords were homogenized in ice-cold RIPA lysis buffer (Sigma) supplemented with protease (Sigma, USA) and phosphatase inhibitor (Roche, USA) cocktails. After centrifugation, protein concentration in supernatants was measured with the Pierce BCA protein assay kit (Thermo Scientific, USA). Samples from 12 week and end-stage groups containing equal amounts of protein were then used for measuring the expression of the pro-inflammatory cytokine TNF-α (LSBio, USA, mouse ELISA Kit) and IL-1β (R&D System mouse IL-1β ELISA Kit) following the manufacturer's protocol. For the end-stage group, spinal cord lysates from 24-week old WT mice were used as the control group. Levels of cytokines are expressed as pg/ml and mean values were compared between genotypes.

2.4. Western blot analysis

Immunoblotting was performed on lysates from lumbar spinal cords dissected from WT, SOD1 and SOD1T1 KO mice at 12 weeks of age. Samples were homogenized in RIPA lysis buffer (Millipore, USA) with a protease (Sigma, USA) and phosphatase (Roche, USA) inhibitor cocktail. Protein concentration was determined using the Pierce BCA protein estimation kit (Thermo Scientific, USA). Samples were then separated by SDS-PAGE, transferred onto PVDF membranes (Life Technologies, USA) that were then blocked in 5% BSA in TBST. Primary antibodies were: Rabbit monoclonal anti TNF-R1 (1:1000, Cell Signaling); mouse monoclonal anti-VEGF (1:1000, SantaCruz) and Rabbit anti-nitrotyrosine antibody (1:500, Millipore). Membranes were then incubated with the specific HRP-conjugated secondary antibodies and the signal generated by the ECL reagent (GE Healthcare) was detected with a Syngene Bio-Imaging System. β-actin served as a loading control using Anti-β-actin HRP (1:5000, SantaCruz).

2.5. Evaluation of motor performance

Muscle strength and coordination were assessed by an accelerating rota-rod (Ugo Basile, Italy) that rotates from 4 to 40 RPM over 5 min as previously described (Yanpallewar et al. 2012). After two training trials of 5 min each (at 11 weeks) animals were run three times a week (Monday, Wednesday, Friday from 12 weeks on) and the duration for which the animal stayed on the rota-rod without falling (up to a maximum of 300 s) was recorded (Yanpallewar et al. 2012).

3. Analysis of disease progression and survival

To monitor the progression of the disease we used two different parameters: early progression of disease and end-stage disease in the animals. Starting at 8 weeks of age, animals were weighed three times weekly (Monday, Wednesday, Friday). Given that animals start losing weight with disease progression, we defined the early progression of disease as the duration between the time of peak weight and the time when animals lose 10% of peak weight due to muscle atrophy. End-stage was defined as the age of actual death of the animal

or the age at which paralysis rendered the animal unable to right itself within 20 s when placed on its side (Boillee et al. 2006b; Tan et al. 2020; Yanpallewar et al. 2012).

3.1. β-Galactosidase staining

After perfusion of the animals, lumbar spinal cords were dissected, post-fixed in 4% PFA for 2 h and cryoprotected overnight in PBS containing 30% sucrose. Cryostat sections (50 μm) were then stained by incubation overnight at 32 °C in a 4 mg/ml X-Gal, 5 mM potassium ferrocyanide, 5 mM potassium ferricyanide, 2 mM $MgCl_2$ and 0.25% Triton X-100 solution in PBS. All chemicals were from Sigma-Aldrich (USA).

3.2. Evaluation of calcium transients in astrocytes

Mouse astrocytes were obtained by enzymatic digestion of E18 embryonic cortex cultured for 7–10 days. For calcium transients recording astrocytes were plated on round coverslip (5 mm diameter) and loaded with 1 micromolar Indo-1-AM (life technology) for 1 h in the presence of Pluronic® surfactant (Life Technology 1/100) and probenecid (Life Technology 2 mM). After washing, cells were incubated at 37 °C, 5% CO_2 for at least 30 min to allow de-esterification. Coverslips were then transferred to the stage of an Axioskop2FS and superfused with recording buffer [NaCl 135 mM, KCl 5 mM, $MgSO_4$ 1.2 mM, $CaCl_2$ 2.5 mM, Hepes 5 mM, and glucose 10 mM (pH 7.4; 300 mOsm, 27 °C)]. Calcium transients were evoked by brief (100 ms) pressure steps (50 hPa) applied to a 1–2 μm tip pipette filled with recording buffer containing 100 ng/ml BDNF. For negative control, the pipet was filled with recording buffer containing BDNF denatured at 95 °C for 5 min. Fluorescence at 405 and 480 nm elicited by a 350 nm light pulse (20 s) was recorded by a photomultiplier (TILL Photonics), digitized and stored in a PC (Digidata 1322, PClamp 9 Axon, CA). F1/F2 ratio was calculated and used for calculation of Ca^{2+}. Instrument calibration was performed with ionophore and calcium calibration buffer following the manufacturer instructions (Life Technology).

3.3. Statistical analysis

Comparisons of motor neuron numbers and rotarod performance between the groups at 12 weeks of age were done by one-way ANOVA followed by post-hoc Tukey's or Dunn's multiple comparison tests. Survival analysis (for early progression of disease and end stage) was subjected to Kaplan-Meier Statistics. Differences in mean values for survival analysis were subjected to Student '*t*' test. A Logrank *P* values was calculated to compare the survival curves. GraphPad Prism software (USA) was used for all statistical analysis.

4.   Results

4.1.   TrkB.T1 is widely expressed in the spinal cord

TrkB receptors are highly expressed in the mammalian spinal cord and both TrkB.Kin and TrkB.T1 are dynamically regulated during development (Zhang and Huang 2006). While TrkB.Kin has been convincingly reported in motoneurons, the cellular distribution of TrkB. T1 has remained elusive because there are no sensitive antibodies for immunohistochemical analysis (Josephson et al. 2001). To characterize the cellular expression of TrkB.T1 in the spinal cord we have employed a mouse model with a knock-in V5 tag (14 aa epitope of

paramyxovirus SV5 protein) inserted in frame before the TrkB.T1 stop codon that faithfully recapitulates TrkB.T1 expression [(TrkB.T1-V5) (Fulgenzi et al. 2020)]. We anticipated that staining of TrkB.T1-V5 adult mouse spinal cords with an anti-V5 antibody would reveal a discrete cell-specific pattern of TrkB.T1 expression. Surprisingly, the staining showed diffuse, non-cell specific expression of TrkB.T1 in both the dorsal and ventral lumbar spinal cord (Fig. 1). Consistent with earlier Western blot analysis data (Zhang and Huang 2006) TrkB.T1 levels appear higher in mature (12 WK) as compared to young animals (p17). Nevertheless, the cellular pattern of expression is similar over time (Fig. 1). These data suggest that TrkB.T1 is expressed ubiquitously across diverse cell types in the spinal cord and its overall spatial distribution does not change during post-natal development.

4.2. BDNF-induced calcium transients are not affected by mutant SOD1 protein in astrocytes

Neuro-inflammation is one of the characteristic features of ALS, seen in all patients as well as ALS mouse models, that contributes significantly to disease progression (McCauley and Baloh 2019). For example, reactive microglia cells and astrocytes release pro-inflammatory cytokines, free radicals, glutamate and pro-apoptotic factors that contribute to motoneuron death (Agulhon et al. 2008). Mechanistically, the release of these toxic factors is mediated by vesicular SNARE proteins (Kawamata et al. 2014) whose activity is associated with increased levels of intracellular calcium. The most widely accepted mechanism for astrocytic Ca^{2+} increases is through G-protein coupled receptor (GPCR) activation of the canonical phospholipase C (PLC)/inositol 1,4,5-trisphosphate (IP3) pathway leading to IP3 receptor (IP3R) activation and Ca^{2+} release from the endoplasmic reticulum (ER). Since Ca^{2+} release from astrocytic calcium stores is also activated by BDNF through the TrkB.T1 receptor (Rose et al. 2003), we first investigated whether TrkB.T1 deletion can influence calcium release from intracellular stores in response to BDNF in WT, SOD1, SOD1-TrkB.T1 KO and TrkB.T1 KO mice. Astrocytes of each genotype were isolated from embryonic day 18 (E18) pups and cultured over a period of about 10 days to allow maturation and up-regulation of TrkB.T1 (Holt et al. 2019). Astrocytes from all genotypes had similar morphology since they were cultured in the absence of BDNF to record calcium transients in response to acute BDNF stimulation (Fig. 2). Analysis of the recordings revealed that deletion of TrkB.T1 in WT as well as SOD1 mutant mice completely abolished BDNF-induced release of calcium from intracellular stores in astrocytes. Interestingly, we found that both control and SOD1 mutant astrocytes respond to BDNF stimulation. However, there was a slight increase in the BDNF-induced calcium transients in the SOD1 mutant astrocytes suggesting that SOD1 mutants may be more excitable (Fig. 2D).

4.3. TrkB.T1 deletion does not influence reactive gliosis levels in SOD1G93A mutant mice

To investigate whether BDNF-TrkB.T1 signaling contributes to the reactive gliosis reported in the SOD1G93A mutant spinal cords, we looked for changes in activated microglia and astrocytes by Iba1 (activated microglial marker) and GFAP (astrocytic marker) immunofluorescence analysis. As previously reported (Boillee et al. 2006b), we observed significant microgliosis in the lumbar spinal cord of SOD1 mutant mice at 12 weeks of age when compared to WT control mice (Fig. 3). Deletion of TrkB.T1, however, did not alter the levels of Iba1 immunoreactive microglia induced by mutant SOD1 protein (Fig. 3

A–F). Similarly, we also observed a significant astrocytosis in SOD1 mutant mice (Fig. 3 I, J) that was not affected by TrkB.T1 deletion (Fig. 3K, L). These results suggest that BDNF-TrkB.T1 signaling does not alter the SOD1G93A mutant reactive gliosis (Fig. 3M, N). Since reactive microglia cells and astrocytes release pro-inflammatory cytokines, we further tested whether TrkB.T1 influences the inflammatory response of mutant mice by investigating lumbar spinal cord levels of tumor necrosis factor alfa (TNFα) and interleukin-1β (IL-1β), cytokines commonly detected during inflammation (Jeyachandran et al. 2015; Zou et al. 2020). However, at early stages of the disease, when TrkB.T1 deletion delays motoneurons cell death caused by the SOD1 mutant protein (12 WK), there were no differences in either TNFα or IL-1β levels across genotypes suggesting that these cytokines are not involved in the early phase of motoneuron cell death (Fig. 4A, C). Nevertheless, as expected, by end stage disease, SOD1 mice had significantly higher levels of both cytokines compared to controls. Importantly, these levels were comparable between SOD1 and SOD1-TrkB.T1 KO mice suggesting that TrkB. T1 deletion does not influence the overall levels of TNFα and IL-1β caused by accumulation of SOD1 mutant protein (Fig. 4B, D). TNF receptor 1 levels were also not different between genotypes at 12 WK, although some mutant mice had higher levels of this receptor (Fig. 4E). Nevertheless, again we found that, although TNF-R1 was consistently upregulated at the end stage disease, there were no differences between SOD1 and SOD1-TrkB.T1 KO mice (Fig. 4F–G). To test whether loss of BDNF-TrkB.T1 signaling has an effect on other growth factor-activated signaling pathways in ALS, we investigated the levels of vascular endothelial growth factor (VEGF), a potent pro-survival growth factor that is upregulated in the spinal cord of ALS models at both onset and end stage disease (Nikodemova et al. 2014). However, while we confirmed that VEGF is upregulated in 12 WK and end stage SOD1G93A spinal cords, we found that deletion of TrkB.T1 did not influence its levels in the SOD1 mutant mice (Fig. 4E, F, H).

In an experimental autoimmune encephalomyelitis (EAE) mouse model it has been reported that TrkB.T1 stimulates astrocytes to release nitric oxide (NO) leading to neuronal damage while astrocyte deletion of TrkB protects from EAE-induced neurodegeneration.

(Colombo et al. 2012). To test whether changes in NO activity levels are influenced by TrkB.T1 in SOD1 mutant mice we analyzed NO signaling pathway at the early stages of disease. Expression of iNOS in ventral lumbar spinal cords by immunofluorescence failed to detect any motor neuron specific iNOS immunoreactivity Fig.(5A, C, E). To overcome the potential inability to detect iNOS because it is either transient, unstable or below the threshold limit of detection we next analyzed the expression of nitrotyrosine, an indicator of nitration of protein tyrosine residues, and the levels of nitrates/nitrites which are the final products of the nitric oxide pathway (Drechsel et al. 2012). Lumbar spinal cord immunofluroscence analysis showed nitrotyrosine immunoreactivity in motor neurons as well as in other cells of the ventral spinal cord (Fig. 5B, D, F). However, there were no obvious significant differences between genotypes. Similarly, lumbar spinal cord Western blot analysis showed several 15 to 80 kDa proteins with nitration of tyrosine residues but did not show any difference between mutant and control mice (Fig. 5G). Lastly, colorimetric measurements of nitrates/nitrites also showed no increase in the levels of these inorganic anions in the SOD1 mutant lumbar spinal cords compared to control and SOD1T1 KO mice (Fig. 5H). Together, these data suggest that the nitric oxide signaling pathway is not

affected in the SOD1 mutant mice during the early stages of disease at the time we see a neuroprotective role of the TrkB.T1 deletion.

4.4.   Astrocyte-specific deletion of TrkB.T1 in SOD1 mutant mice provides neuroprotection at the early stages of disease

In order to investigate whether the neuroprotective effect caused by global TrkB.T1 deletion (Yanpallewar et al. 2012) is cell-type specific, we used the GFAP- and HB9-cre transgenic mice to delete TrkB.T1 in astrocytes and motoneurons, respectively. Testing of these cre transgenics with the ROSA26-LacZ reporter mouse line verified beta-galactosidase staining (Fig. 6A–C) in lumbar spinal cord astrocytes with the GFAP-cre mouse (Fig. 6C), and motor neurons with the HB9-cre mouse (Fig. 6B). Since TrkB.T1 KO heterozygosis is not haploinsufficient (Carim-Todd et al. 2009), to increase the efficiency of the cell type-specific deletion we combined the specific cre transgene and a conditional TrkB.T1 allele with a TrkB.T1 KO heterozygous allele. Mutant and control mice generated by crossing these cre lines with the SOD1 mutation and the TrkB.T1 conditional allele were then analyzed by Nissl staining and stereological quantification of lumbar spinal cord motor neuron number (Fig. 6D–I). At 12 weeks of age SOD1 mutant mice showed a significant loss of motor neurons that was partially rescued by complete TrkB.T1 deletion, as previously reported ((Yanpallewar et al. 2012); Fig. 6D–F and I, number of motor neurons: 4803 ± 178.7 in WT, 3597 ± 174.4 in SOD1 and 5098 ± 318.7 in SOD1T1 KO mice, $p < 0.05$). However, motor neuron specific deletion of TrkB.T1 did not offer any protection against motor neuron loss (Fig. 6H–I, 3516 ± 175.5 in SOD1T1 HB9), while an intermediate number of surviving motor neurons were observed when TrkB.T1 was deleted in astrocytes but without reaching statistical significance compared to WT or SOD1 mutant mice (Fig. 6G, I; 3978 ± 200.7 in SOD1T1GFAP mice).

We then tested the mice for motor performance an accelerating rota-rod over a period of 5 min. Performance of SOD1 mutant mice compared to control mice was significantly impaired, as expected (Fig. 7A, 249.1 ± 5.8 s in WT vs. 213.9 ± 6.7 in SOD1 mutant mice, $p < 0.05$). Interestingly, either complete KO or astrocyte-specific deletion of TrkB.T1 rescued the motor performance of SOD1 mutant mice (Fig. 7A, 254.2 ± 9.2 in SOD1T1 KO and 240.3 ± 6 in SOD1T1 GFAP mice). In contrast, there was no observable difference in the rota-rod performance of SOD1 mutant mice with motor neuron specific deletion of TrkB.T1 (Fig. 7A, 187.8 ± 12.6 s, $p > 0.05$).

Next we tested the progression of disease and overall life span of SOD1 mutant mice with astrocyte-specific deletion of TrkB.T1 (Fig. 7B, C). The duration of the early phase of the disease was the time between the peak body weight to when the mice lose 10% of their weight (Boillee et al. 2006b; Tan et al. 2020; Yanpallewar et al. 2012). We found that astrocyte specific deletion of TrkB.T1 extends the mean duration of the early phase by 7 days (a 28% increase) in SOD1 mutant mice. (Fig. 7B, 32.75 ± 1.9 days SOD1T1 GFAP and 25.44 ± 2.7 days in SOD1 mice, $p = 0.0301$ by one tailed t-test). However, analysis of the mean lifespan of these mutants did not show any difference between genotypes as also reported for SOD1 mutants with complete deletion of TrkB.T1 [Fig. 7C (Yanpallewar et al. 2012)].

5. Discussion

We have investigated the role of BDNF-TrkB.T1 in the pathophysiology of ALS using the SOD1 G93A mouse mutant as a model. The question is relevant because BDNF has been used in human ALS clinical trials but has failed to show efficacy in slowing disease progression (Beck et al. 2005; Group, 1999; Kalra et al. 2003; Ochs et al. 2000). The causes of the failure are still unknown but have been attributed, at least in part, to poor pharmacokinetics and limited diffusion capability due to BDNF physicochemical properties (Henriques et al. 2010; Thoenen and Sendtner 2002). The rationale for supporting the use of BDNF in ALS comes from early work showing that it can rescue axotomized motoneurons and it improves the phenotype of wobbler mutant mice (Ikeda et al. 1995; Sendtner et al. 1992; Yan et al. 1992). In addition, BDNF protects neurons from in vivo excitotoxicity and it prevents cell death of motoneurons in a spinal root avulsion model (Kishino et al. 1997; Wu et al. 2003). However, to our knowledge there is no clear data showing that increasing BDNF/TrkB signaling is beneficial in more relevant mouse models of ALS such as the SOD1 G93A mouse mutant. Our study provides direct evidence that BDNF/TrkB signaling affects the pathophysiology of ALS in a relevant mouse model of human motoneuron degeneration.

An important question that arises from our findings is regarding the mechanism by which deletion of TrkB.T1 delays motoneuron cell death. It had been reported that, in the spinal cord, TrkB.T1 is significantly upregulated post-natally and into adulthood (Zhang and Huang 2006). However, the lack of specific antibodies for the TrkB.T1 isoform has prevented the identification of the specific cell type/s expressing this isoform. By using a mouse model with a genetically tagged endogenous TrkB.T1 we have shown that TrkB.T1 is expressed in virtually all cell types of the spinal cord [(Fulgenzi et al. 2020); Fig. 1]. This information prompted us to test the potential role of TrkB.T1 in regulating the inflammatory response to the mutant SOD1 protein and the possibility of a cell autonomous function in glial and motoneuron cells. The finding that BDNF-induced calcium transients were slightly increased in SOD1 mutant as compared to WT astrocytes suggested increased excitability and a possible role of TrkB.T1 in the inflammatory response in mutant spinal cord. However, analysis of several markers such as GFAP, Iba1, the cytokines TNFα and IL-1β and the iNOS pathway did not show any significant change in SOD1 mutant mice lacking TrkB.T1 (Drechsel et al. 2012; Jeyachandran et al. 2015). This suggests that TrkB.T1 regulation of calcium signaling may not have a direct role in the inflammatory response associated with the pathogenesis of ALS and the use of TrkB agonists may have limited impact on intrinsic TrkB.T1 signaling and inflammation. Analysis of the growth factor VEGF levels showed upregulation at both 12 WK and end stage in SOD1 mutant spinal cords but deletion of TrkB.T1 did not cause any further changes in its levels suggesting also a lack of cross-talk between the BDNF-TrkB.T1 and the VEGF signaling pathway.

TrkB.T1 specific deletion in motoneurons does not have any effect on the rescue of motoneuron cell death or motor-behavior deficits indicating that expression of TrkB.T1 does not have a significant dominant-negative role on TrkB.FL function as reported for hippocampal neurons (Dorsey et al. 2006; Tomassoni-Ardori et al. 2019). Whether this lack of rescue is caused by deficits in other neurons of the motor system such as spinal cord

interneurons and cortical motor neurons is unclear. However, our strategy showed that, at least in spinal motor neurons, deletion of TrkB.T1 is not sufficient to alter motor neuron survival and function caused by mutant SOD1 protein.

One of the most interesting finding of this study is that TrkB.T1 knockout in astrocytes using the GFAP-cre transgene preserves muscle strength and co-ordination at early stages of disease (Fig. 7). Since this rescue is not attributable to change in spinal cord inflammatory status, one possibility was that GFAP-cre expression in other cell populations such as Schwann cells, which are important for myelination of motor neuron axons and formation of neuromuscular junctions may contribute to the rescue. However, the lack of motor-coordination deficits in TrkB.T1 deficient mice (Carim-Todd et al. 2009) and the report that specific overexpression of SOD1G93A mutant in Schwann cells is not pathological to spinal motor neurons suggests that this may not be the case (Turner et al. 2010). Therefore, a more plausible hypothesis is that widespread expression of TrkB.T1 may limit BDNF trophic activity in diseased motoneurons (Fig. 1). Indeed, BDNF administered by intra-cerebroventricular infusion does not penetrate the brain and localizes predominantly to the ependymal lining with limited penetration into the subjacent neural parenchyma. The ependymal distribution of the infused BDNF overlaps with TrkB.T1 expression suggesting that truncated TrkB provides a barrier to BDNF diffusion (Biffo et al. 1995; Morse et al. 1993). This might also explain how even intrathecal injection of BDNF failed to improve ALS outcome in clinical trials (Beck et al. 2005; Kalra et al. 2003). Conversely, NGF injected at similar concentrations diffuses and reaches septal neurons more effectively because its receptor, TrkA, does not have truncated isoforms and has more limited expression in the CNS (Morse et al. 1993). These results raise the question of how to facilitate the delivery of BDNF trophic activity to motoneurons or other CNS neuronal populations that are surrounded by cells expressing TrkB.T1 (Fig. 1). Pharmacological agents such as the adenosine A2A receptor agonist CGS21680, can activate motoneuron TrkB receptor signaling independent of neurotrophins by a transactivation mechanism (Wiese et al. 2007; Yanpallewar et al. 2012). However, this strategy is less efficient than neurotrophins in activating TrkB signaling and the rescue is only partial, suggesting that strategies aimed at identifying molecules with BDNF mimetic activities may be more efficient. Significant efforts have been directed toward the generation of agonistic antibodies binding TrkB (Guo et al. 2019; Lin et al. 2008; Merkouris et al. 2018; Qian et al. 2006; Todd et al. 2014; Traub et al. 2017). However, a major challenge is how to efficiently deliver these agonists to their target. Recently it has been reported that a TrkB agonist antibody has superior tissue penetration over BDNF (Guo et al. 2019). This enhanced diffusion property has been attributed to the reduced positive charges of antibodies when compared to BDNF and their significantly longer half-life. However, it is unclear whether the low diffusion rate of BDNF in tissues is caused mainly by its strong positive charges. Thus, it appears that TrkB agonist antibodies may have unique properties that allow them to overcome the TrkB.T1 scavenger function. For example, is it possible that agonist antibodies can be selected based on their ability to bind specific isoforms? Although the TrkB gene produces, by alternative splicing, isoforms with genetically identical extracellular domains it would be of interest to investigate whether these isoforms undergo differential post-translational modifications, as suggested for the TrkC receptor isoforms (Brahimi et al. 2020). For

example, analysis of the pattern of glycosylation of different TrkB isoforms may help identify possible epitope differences that can be exploited for the generation of TrkB agonist antibodies. Additionally, TrkB.T1 KO mice could provide a tool for the identification of TrkB agonist antibodies whose brain diffusion ability is not affected by the presence or absence of TrkB.T1 receptors with the potential to be used for intrathecal infusion in clinical trials.

In summary, our finding that astrocytes-specific deletion of TrkB.T1 partially improves motor performance and delays progression of the early phase of disease supports the notion that reducing TrkB.T1 levels in astrocytes may be beneficial (Fig. 7). Further work will be needed to determine what other cell types expressing TrkB.T1 may influence diseased motoneurons. Nevertheless, our results suggest that enhancing BDNF/TrkB.kin signaling is beneficial in an ALS mouse model and provides information that can be useful for instructing future clinical trials aimed at increased signaling of this pathway to improve motoneuron survival.

Acknowledgements

References

Agulhon C, Petravicz J, McMullen AB, Sweger EJ, Minton SK, Taves SR, Casper KB, Fiacco TA, McCarthy KD, 2008. What is the role of astrocyte calcium in neurophysiology? Neuron. 59, 932–946. [PubMed: 18817732]

Beck M, Flachenecker P, Magnus T, Giess R, Reiners K, Toyka KV, Naumann M, 2005. Autonomic dysfunction in ALS: a preliminary study on the effects of intrathecal BDNF. Amyotroph. Later. Scler. Other Motor Neuron Disord. 6, 100–103.

Biffo S, Offenhauser N, Carter BD, Barde YA, 1995. Selective binding and internalisation by truncated receptors restrict the availability of BDNF during development. Development. 121, 2461–2470. [PubMed: 7671810]

Boillee S, Vande Velde C, Cleveland DW, 2006a. ALS: a disease of motor neurons and their nonneuronal neighbors. Neuron. 52, 39–59. [PubMed: 17015226]

Boillee S, Yamanaka K, Lobsiger CS, Copeland NG, Jenkins NA, Kassiotis G, Kollias G, Cleveland DW, 2006b. Onset and progression in inherited ALS determined by motor neurons and microglia. Science. 312, 1389–1392. [PubMed: 16741123]

Brahimi F, Galan A, Jmaeff S, Barcelona PF, De Jay N, Dejgaard K, Young JC, Kleinman CL, Thomas DY, Saragovi HU, 2020. Alternative splicing of a receptor intracellular domain yields different Ectodomain conformations, enabling isoform-selective functional ligands. iScience. 23, 101447. [PubMed: 32829283]

Buck CR, Seburn KL, Cope TC, 2000. Neurotrophin expression by spinal motoneurons in adult and developing rats. J. Comp. Neurol. 416, 309–318. [PubMed: 10602090]

Carim-Todd L, Bath KG, Fulgenzi G, Yanpallewar S, Jing D, Barrick CA, Becker J, Buckley H, Dorsey SG, Lee FS, Tessarollo L, 2009. Endogenous truncated TrkB.T1 receptor regulates neuronal complexity and TrkB kinase receptor function in vivo. J. Neurosci. 29, 678–685. [PubMed: 19158294]

Chao MV, Rajagopal R, Lee FS, 2006. Neurotrophin signalling in health and disease. Clin. Sci. 110, 167–173.

Colombo E, Cordiglieri C, Melli G, Newcombe J, Krumbholz M, Parada LF, Medico E, Hohlfeld R, Meinl E, Farina C, 2012. Stimulation of the neurotrophin receptor TrkB on astrocytes drives nitric oxide production and neurodegeneration. J. Exp. Med. 209, 521–535. [PubMed: 22393127]

Dorsey SG, Renn CL, Carim-Todd L, Barrick CA, Bambrick L, Krueger BK, Ward CW, Tessarollo L, 2006. In vivo restoration of physiological levels of truncated TrkB.T1 receptor rescues neuronal cell death in a trisomic mouse model. Neuron. 51, 21–28. [PubMed: 16815329]

Dorsey SG, Lovering RM, Renn CL, Leitch CC, Liu X, Tallon LJ, Sadzewicz LD, Pratap A, Ott S, Sengamalay N, Jones KM, Barrick C, Fulgenzi G, Becker J, Voelker K, Talmadge R, Harvey BK, Wyatt RM, Vernon-Pitts E, Zhang C, Shokat K, Fraser-Liggett C, Balice-Gordon RJ, Tessarollo L, Ward CW, 2012. Genetic deletion of trkB.T1 increases neuromuscular function. Am. J. Phys. Cell Phys. 302, C141–C153.

Drechsel DA, Estevez AG, Barbeito L, Beckman JS, 2012. Nitric oxide-mediated oxidative damage and the progressive demise of motor neurons in ALS. Neurotox. Res. 22, 251–264. [PubMed: 22488161]

Fulgenzi G, Tomassoni-Ardori F, Babini L, Becker J, Barrick C, Puverel S, Tessarollo L, 2015. BDNF modulates heart contraction force and long-term homeostasis through truncated TrkB.T1 receptor activation. J. Cell Biol. 210, 1003–1012. [PubMed: 26347138]

Fulgenzi G, Hong Z, Tomassoni-Ardori F, Barella LF, Becker J, Barrick C, Swing D, Yanpallewar S, Croix BS, Wess J, Gavrilova O, Tessarollo L, 2020. Novel metabolic role for BDNF in pancreatic beta-cell insulin secretion. Nat. Commun. 11, 1950. [PubMed: 32327658]

Gravel C, Gotz R, Lorrain A, Sendtner M, 1997. Adenoviral gene transfer of ciliary neurotrophic factor and brain-derived neurotrophic factor leads to long-term survival of axotomized motor neurons. Nat. Med. 3, 765–770. [PubMed: 9212104]

Group BS, 1999. A controlled trial of recombinant methionyl human BDNF in ALS: the BDNF study group (phase III). Neurology. 52, 1427–1433. [PubMed: 10227630]

Guo W, Pang K, Chen Y, Wang S, Li H, Xu Y, Han F, Yao H, Liu H, Lopes-Rodrigues V, Sun D, Shao J, Shen J, Dou Y, Zhang W, You H, Wu W, Lu B, 2019. TrkB agonistic antibodies superior to BDNF: utility in treating motoneuron degeneration. Neurobiol. Dis. 132, 104590. [PubMed: 31470106]

Henriques A, Pitzer C, Schneider A, 2010. Neurotrophic growth factors for the treatment of amyotrophic lateral sclerosis: where do we stand? Front. Neurosci. 4, 32. [PubMed: 20592948]

Holt LM, Hernandez RD, Pacheco NL, Torres Ceja B, Hossain M, Olsen ML, 2019. Astrocyte morphogenesis is dependent on BDNF signaling via astrocytic TrkB. T1. Elife 8.

Huang EJ, Reichardt LF, 2001. Neurotrophins: roles in neuronal development and function. Annu. Rev. Neurosci. 24, 677–736. [PubMed: 11520916]

Huang EJ, Reichardt LF, 2003. Trk receptors: roles in neuronal signal transduction. Annu. Rev. Biochem. 72, 609–642. [PubMed: 12676795]

Ikeda K, Klinkosz B, Greene T, Cedarbaum JM, Wong V, Lindsay RM, Mitsumoto H, 1995. Effects of brain-derived neurotrophic factor on motor dysfunction in wobbler mouse motor neuron disease. Ann. Neurol. 37, 505–511. [PubMed: 7717687]

Jeyachandran A, Mertens B, McKissick EA, Mitchell CS, 2015. Type I vs. type II cytokine levels as a function of SOD1 G93A mouse amyotrophic lateral sclerosis disease progression. Front. Cell. Neurosci. 9, 462. [PubMed: 26648846]

Josephson A, Widenfalk J, Trifunovski A, Widmer HR, Olson L, Spenger C, 2001. GDNF and NGF family members and receptors in human fetal and adult spinal cord and dorsal root ganglia. J. Comp. Neurol. 440, 204–217. [PubMed: 11745618]

Kalra S, Genge A, Arnold DL, 2003. A prospective, randomized, placebo-controlled evaluation of corticoneuronal response to intrathecal BDNF therapy in ALS using magnetic resonance spectroscopy: feasibility and results. Amyotroph. Later. Scler. Other Motor Neuron Disord. 4, 22–26.

Kaplan DR, Miller FD, 2000. Neurotrophin signal transduction in the nervous system. Curr. Opin. Neurobiol. 10, 381–391. [PubMed: 10851172]

Katz JS, Barohn RJ, Dimachkie MM, Mitsumoto H, 2015. The dilemma of the clinical Trialist in amyotrophic lateral sclerosis: the hurdles to finding a cure. Neurol. Clin. 33, 937–947. [PubMed: 26515630]

Kawamata H, Ng SK, Diaz N, Burstein S, Morel L, Osgood A, Sider B, Higashimori H, Haydon PG, Manfredi G, Yang Y, 2014. Abnormal intracellular calcium signaling and SNARE-dependent exocytosis contributes to SOD1G93A astrocyte-mediated toxicity in amyotrophic lateral sclerosis. J. Neurosci. 34, 2331–2348. [PubMed: 24501372]

Kishino A, Ishige Y, Tatsuno T, Nakayama C, Noguchi H, 1997. BDNF prevents and reverses adult rat motor neuron degeneration and induces axonal outgrowth. Exp. Neurol. 144, 273–286. [PubMed: 9168829]

Kust BM, Copray JC, Brouwer N, Troost D, Boddeke HW, 2002. Elevated levels of neurotrophins in human biceps brachii tissue of amyotrophic lateral sclerosis. Exp. Neurol. 177, 419–427. [PubMed: 12429188]

Lin JC, Tsao D, Barras P, Bastarrachea RA, Boyd B, Chou J, Rosete R, Long H, Forgie A, Abdiche Y, Dilley J, Stratton J, Garcia C, Sloane DL, Comuzzie AG, Rosenthal A, 2008. Appetite enhancement and weight gain by peripheral administration of TrkB agonists in non-human primates. PLoS One 3, e1900. [PubMed: 18382675]

Lu B, Nagappan G, Guan X, Nathan PJ, Wren P, 2013. BDNF-based synaptic repair as a disease-modifying strategy for neurodegenerative diseases. Nat. Rev. Neurosci. 14, 401–416. [PubMed: 23674053]

McCauley ME, Baloh RH, 2019. Inflammation in ALS/FTD pathogenesis. Acta Neuropathol. 137, 715–730. [PubMed: 30465257]

Merkouris S, Barde YA, Binley KE, Allen ND, Stepanov AV, Wu NC, Grande G, Lin CW, Li M, Nan X, Chacon-Fernandez P, DiStefano PS, Lindsay RM, Lerner RA, Xie J, 2018. Fully human agonist antibodies to TrkB using autocrine cell-based selection from a combinatorial antibody library. Proc. Natl. Acad. Sci. U. S. A. 115, E7023–E7032. [PubMed: 29987039]

Mitchell JD, Borasio GD, 2007. Amyotrophic lateral sclerosis. Lancet. 369, 2031–2041. [PubMed: 17574095]

Morse JK, Wiegand SJ, Anderson K, You Y, Cai N, Carnahan J, Miller J, DiStefano PS, Altar CA, Lindsay RM, et al. , 1993. Brain-derived neurotrophic factor (BDNF) prevents the degeneration of medial septal cholinergic neurons following fimbria transection. J. Neurosci. 13, 4146–4156. [PubMed: 8080477]

Mutoh T, Sobue G, Hamano T, Kuriyama M, Hirayama M, Yamamoto M, Mitsuma T, 2000. Decreased phosphorylation levels of TrkB neurotrophin receptor in the spinal cords from patients with amyotrophic lateral sclerosis. Neurochem. Res. 25, 239–245. [PubMed: 10786708]

Nguyen HP, Van Broeckhoven C, van der Zee J, 2018. ALS genes in the genomic era and their implications for FTD. Trends Genet. 34, 404–423. [PubMed: 29605155]

Nikodemova M, Small AL, Smith SM, Mitchell GS, Watters JJ, 2014. Spinal but not cortical microglia acquire an atypical phenotype with high VEGF, galectin-3 and osteopontin, and blunted inflammatory responses in ALS rats. Neurobiol. Dis. 69, 43–53. [PubMed: 24269728]

Ochs G, Penn RD, York M, Giess R, Beck M, Tonn J, Haigh J, Malta E, Traub M, Sendtner M, Toyka KV, 2000. A phase I/II trial of recombinant methionyl human brain derived neurotrophic factor administered by intrathecal infusion to patients with amyotrophic lateral sclerosis. Amyotroph. Later. Scler. Other Motor Neuron Disord. 1, 201–206.

Qian MD, Zhang J, Tan XY, Wood A, Gill D, Cho S, 2006. Novel agonist monoclonal antibodies activate TrkB receptors and demonstrate potent neurotrophic activities. J. Neurosci. 26, 9394–9403. [PubMed: 16971523]

Quarta E, Fulgenzi G, Bravi R, Cohen EJ, Yanpallewar S, Tessarollo L, Minciacchi D, 2018. Deletion of the endogenous TrkB.T1 receptor isoform restores the number of hippocampal CA1 parvalbumin-positive neurons and rescues long-term potentiation in pre-symptomatic mSOD1(G93A) ALS mice. Mol. Cell. Neurosci. 89, 33–41. [PubMed: 29580900]

Rose CR, Blum R, Pichler B, Lepier A, Kafitz KW, Konnerth A, 2003. Truncated TrkB-T1 mediates neurotrophin-evoked calcium signalling in glia cells. Nature. 426, 74–78. [PubMed: 14603320]

Sendtner M, Holtmann B, Kolbeck R, Thoenen H, Barde YA, 1992. Brain-derived neurotrophic factor prevents the death of motoneurons in newborn rats after nerve section. Nature. 360, 757–759. [PubMed: 1465147]

Tan H, Chen M, Pang D, Xia X, Du C, Yang W, Cui Y, Huang C, Jiang W, Bi D, Li C, Shang H, Worley PF, Xiao B, 2020. LanCL1 promotes motor neuron survival and extends the lifespan of amyotrophic lateral sclerosis mice. Cell Death Differ. 27, 1369–1382. [PubMed: 31570855]

Tessarollo L, 1998. Pleiotropic functions of neurotrophins in development. Cytokine Growth Factor Rev. 9, 125–137. [PubMed: 9754707]

Thoenen H, Sendtner M, 2002. Neurotrophins: from enthusiastic expectations through sobering experiences to rational therapeutic approaches. Nat. Neurosci. 5 (Suppl), 1046–1050. [PubMed: 12403983]

Todd D, Gowers I, Dowler SJ, Wall MD, McAllister G, Fischer DF, Dijkstra S, Fratantoni SA, van de Bospoort R, Veenman-Koepke J, Flynn G, Arjomand J, Dominguez C, Munoz-Sanjuan I, Wityak J, Bard JA, 2014. A monoclonal antibody TrkB receptor agonist as a potential therapeutic for Huntington's disease. PLoS One 9, e87923. [PubMed: 24503862]

Tomassoni-Ardori F, Fulgenzi G, Becker J, Barrick C, Palko ME, Kuhn S, Koparde V, Cam M, Yanpallewar S, Oberdoerffer S, Tessarollo L, 2019. Rbfox1 up-regulation impairs BDNF-dependent hippocampal LTP by dysregulating TrkB isoform expression levels. Elife. 8.

Tovar YRLB, Ramirez-Jarquin UN, Lazo-Gomez R, Tapia R, 2014. Trophic factors as modulators of motor neuron physiology and survival: implications for ALS therapy. Front. Cell. Neurosci. 8, 61. [PubMed: 24616665]

Traub S, Stahl H, Rosenbrock H, Simon E, Florin L, Hospach L, Horer S, Heilker R, 2017. Pharmaceutical characterization of tropomyosin receptor kinase B-agonistic antibodies on human induced pluripotent stem (hiPS) cell-derived neurons. J. Pharmacol. Exp. Ther. 361, 355–365. [PubMed: 28351853]

Turner BJ, Ackerley S, Davies KE, Talbot K, 2010. Dismutase-competent SOD1 mutant accumulation in myelinating Schwann cells is not detrimental to normal or transgenic ALS model mice. Hum. Mol. Genet. 19, 815–824. [PubMed: 20008901]

Wiese S, Jablonka S, Holtmann B, Orel N, Rajagopal R, Chao MV, Sendtner M, 2007. Adenosine receptor A2A-R contributes to motoneuron survival by transactivating the tyrosine kinase receptor TrkB. Proc. Natl. Acad. Sci. U. S. A. 104, 17210–17215. [PubMed: 17940030]

Wu W, Li L, Yick LW, Chai H, Xie Y, Yang Y, Prevette DM, Oppenheim RW, 2003. GDNF and BDNF alter the expression of neuronal NOS, c-Jun, and p75 and prevent motoneuron death following spinal root avulsion in adult rats. J. Neurotrauma 20, 603–612. [PubMed: 12906744]

Yan Q, Elliott J, Snider WD, 1992. Brain-derived neurotrophic factor rescues spinal motor neurons from axotomy-induced cell death. Nature. 360, 753–755. [PubMed: 1281520]

Yanpallewar SU, Barrick CA, Buckley H, Becker J, Tessarollo L, 2012. Deletion of the BDNF truncated receptor TrkB.T1 delays disease onset in a mouse model of amyotrophic lateral sclerosis. PLoS One 7, e39946. [PubMed: 22761934]

Zhang J, Huang EJ, 2006. Dynamic expression of neurotrophic factor receptors in postnatal spinal motoneurons and in mouse model of ALS. J. Neurobiol. 66, 882–895. [PubMed: 16680759]

Zou YH, Guan PP, Zhang SQ, Guo YS, Wang P, 2020. Rofecoxib attenuates the pathogenesis of amyotrophic lateral sclerosis by alleviating Cyclooxygenase-2-mediated mechanisms. Front. Neurosci. 14, 817. [PubMed: 32903591]
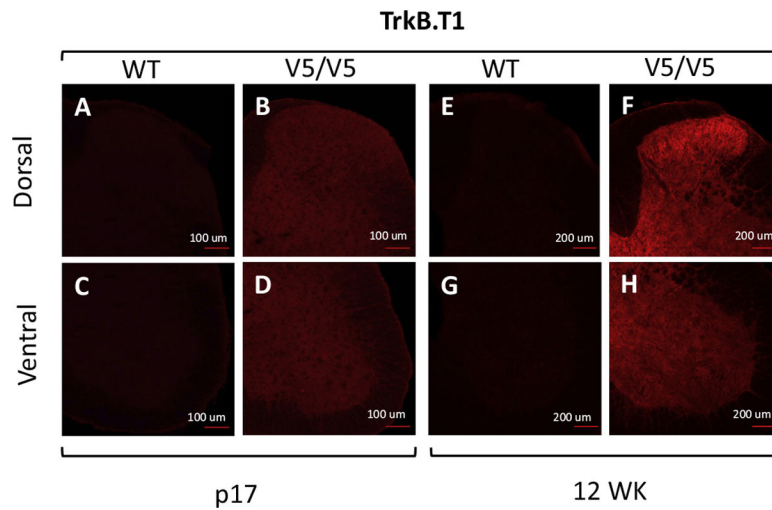
Fig. 1.
TrkB.T1 is widely expressed in post-natal mouse spinal cord. Immunostaining of dorsal (A, B, E, F) and ventral (C, D, G, H) spinal cords from Wild Type (WT; A, C, E, G) and homozygous TrkB.T1-V5 (V5/V5; B, D, F, H) mouse post-natal day 17 (p17) and 12 week-old (12WK) spinal cords stained with an anti-V5 antibody. Note the intense staining indicative of TrkB.T1 expression in virtually all dorsal and ventral spinal cord cells of the transgenic TrkB.T1-V5 mice (B, D, F, H).
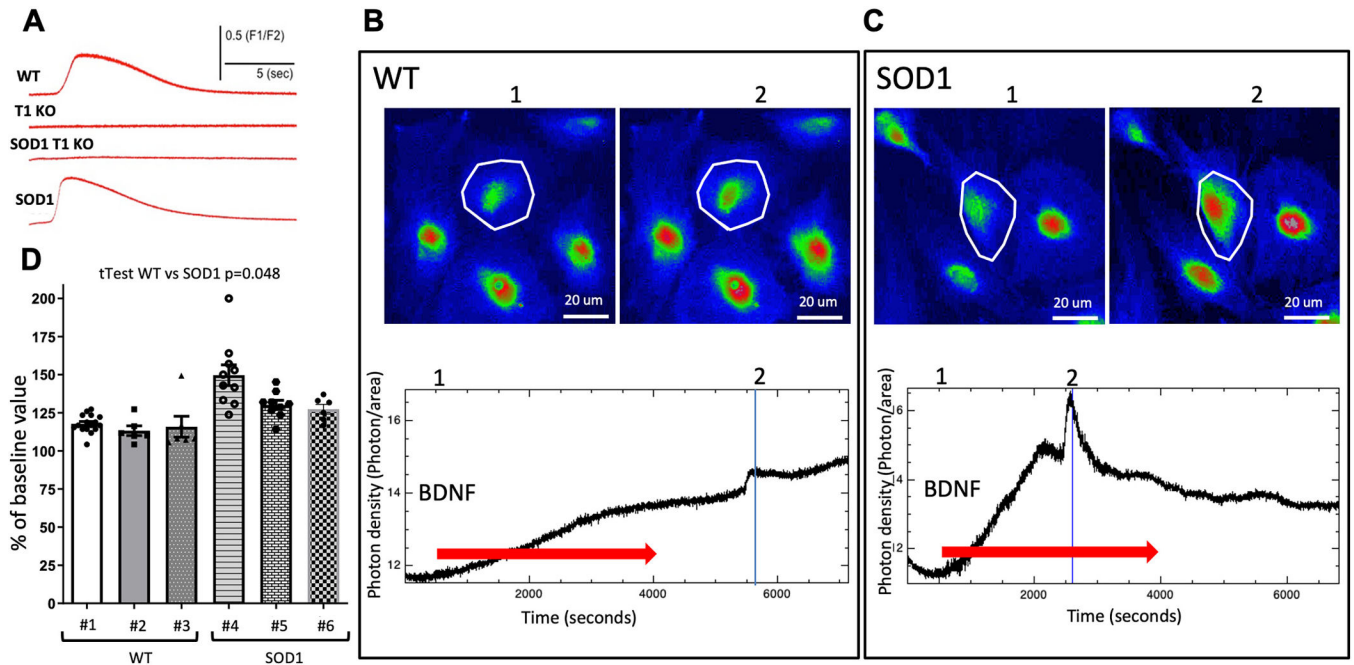
Fig. 2.
Fluo-4 mediated intracellular calcium response to BDNF application in cultured astrocytes.
(A) Astrocytes obtained from E18 embryosmbryos of different genotypes were subjected
to a puff of BDNF and their intracellular calcium levels were recorded. Note the lack of
response to BDNF in both TrkB.T1 KO (T1 KO) as well as SOD1-TrkB.T1 KO (SOD1 T1
KO) astrocytes (A). (B, C) photomicrographs of representative WT and SOD1 astrocytes
before (1) and after (2) BDNF application. Lower panels in B, C show the quantification of
the cell response to BDNF in the boxed areas of the micrographs (Red arrow, continuous
perfusion). Note the higher intracellular calcium elicited by BDNF in the SOD1 astrocytes
is suggestive of a higher basal threshold level of activation. (D) Histogram showing the
quantification of WT and SOD1 astrocytes response to BDNF expressed as percentage of the
change in fluorescence before (1 in B, C) and after (2 in B, C) BDNF application. $N = 28$
cells from 3 independent WT mice (# 1\) and $N = 25$ cells from 3 independent SOD1 mice
(# 4–6).
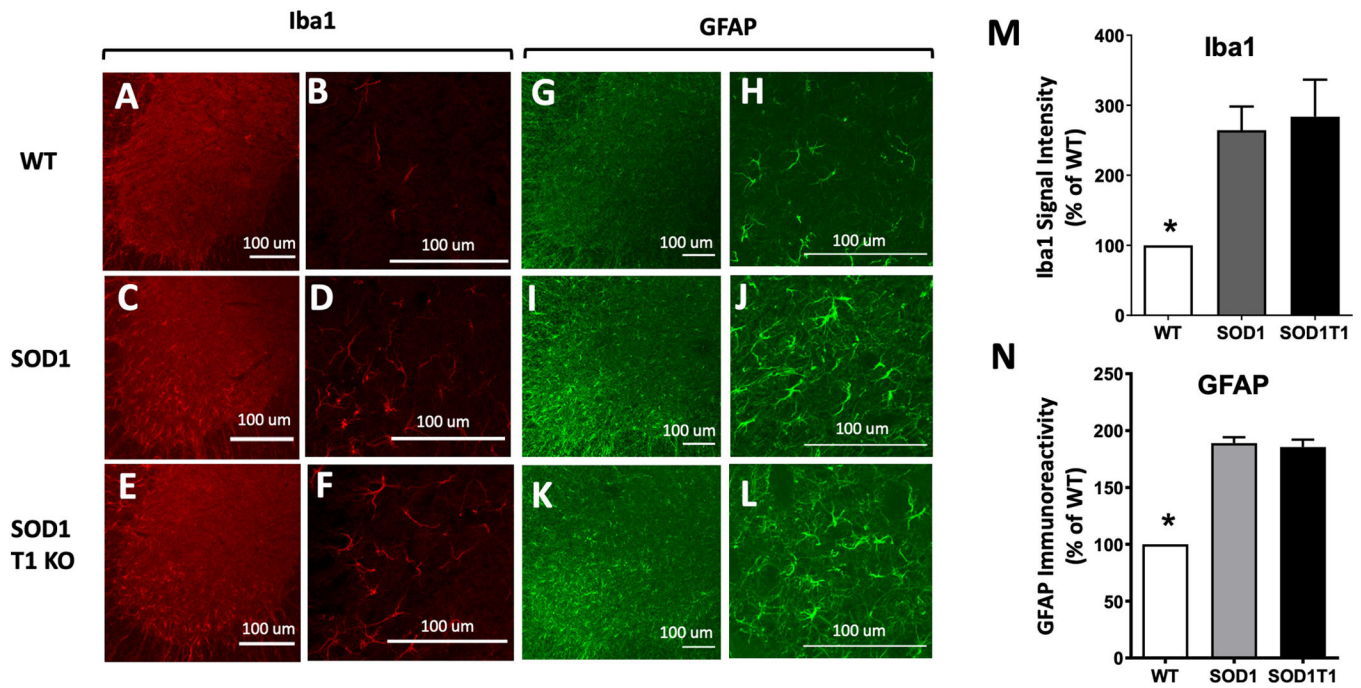
Fig. 3.
Microglial activation and inflammatory astrocytosis in SOD1 mutant mice are not altered
by TrkB.T1 deletion. (A-F) Immunofluorescence images of spinal cord stained with an anti-
Iba1 antibody indicative of microglia activation in WT (A, B), SOD1 (C, D) and SOD1-T1
KO (E, F) 12-week-old mice. (B, D, F) are higher magnification (40×) images for A, C
and E (10× magnification) respectively. (G-L) Immunofluorescence images of spinal cord
stained with an anti-GFAP antibody to detect activated astrocytes in WT (G, H), SOD1 (I, J)
and SOD1-T1 KO (*K,L*) 12 week-old mice. H, J, L are higher magnification (40×) images
of G, I, K (10×) respectively. Note the significant accumulation of GFAP positive cells
in the SOD1 and SOD1-TrkB.T1 mutant ventral lumbar spinal cord (I-L) when compared
to controls (G, H) suggesting that TrkB.T1 deletion does not prevent astrocytosis. (M-N)
Histograms showing quantitative results of Iba1 (M) and GFAP (N) immunoreactivities
between genotypes using NIH Image J software. $N = 5$ per genotype. * indicates $p < 0.05$,
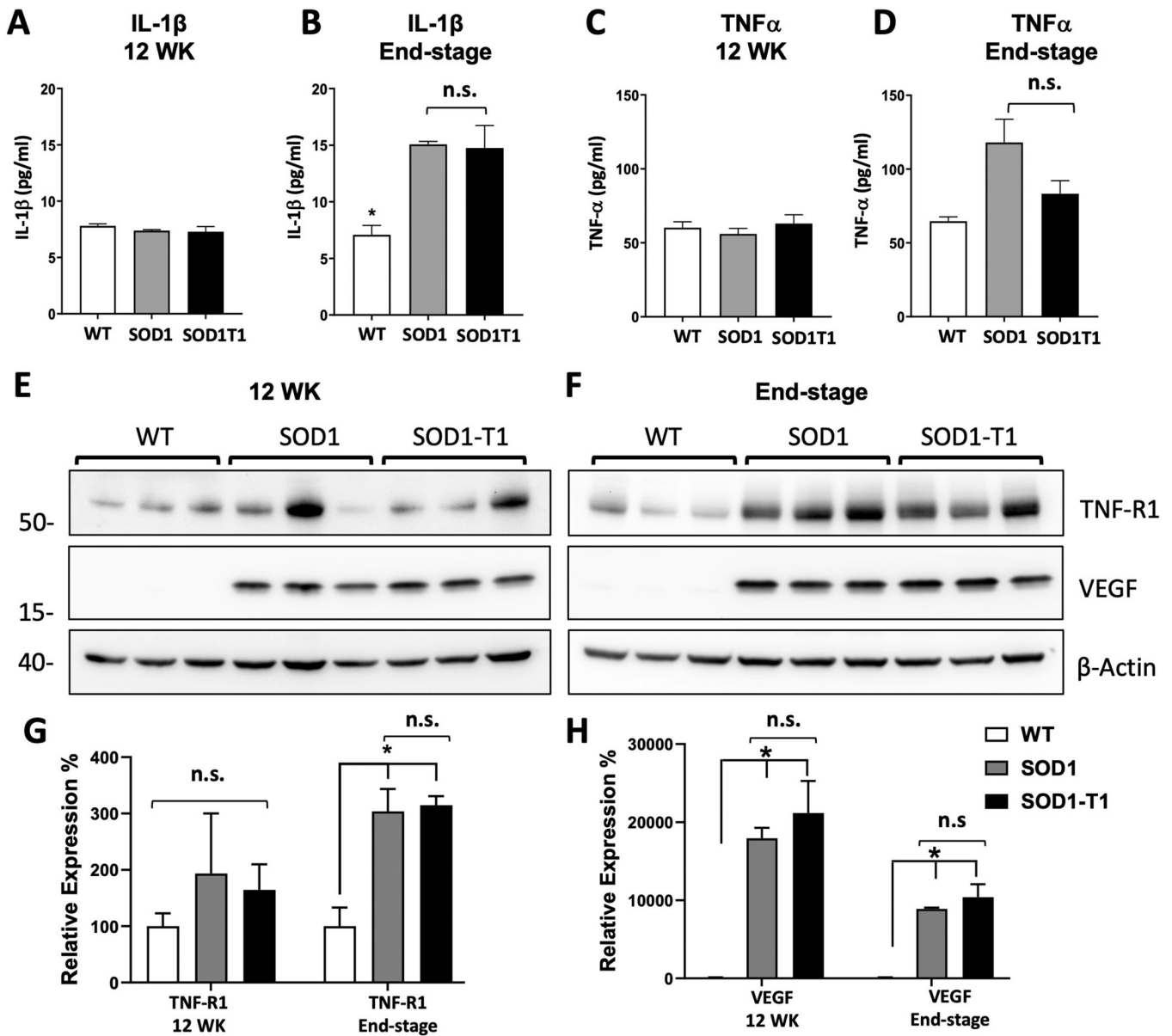ANOVA followed by Tukey Multiple comparison test.

Fig. 4.
TrkB.T1 deletion does not alter the levels of pro-inflammatory cytokines in SOD1 mutant mice. (A-D) ELISA measurement of the pro-inflammatory cytokines TNFα and IL-1β in 12 week (12 WK) and end-stage WT, SOD1 and SOD1-TrkB.T1 KO (SOD1T1) spinal cords. At 12 WK, levels of TNFα (A) and IL-1β (C) did not differ significantly between genotypes ($n = 5$/group) while at end stage, both the SOD1 and SOD1 T1 KO group showed significantly higher levels of TNFα (B) and IL-1β (D) when compared with the WT group ($n = 4$ per group). * indicates $p < 0.05$. Western blot analysis of TNF receptor 1 (TNF-R1) and VEGF at 12 WK and end stage disease (E, F) in control and mutant mice as in A, C. Note that despite some mice show higher levels of TNF-R1 levels at 12 WK there is no difference between groups whereas VEGF is dramatically upregulated in both mutant groups (E). At the end stage, while both TNF-R1 and VEGF are up regulated in mutant
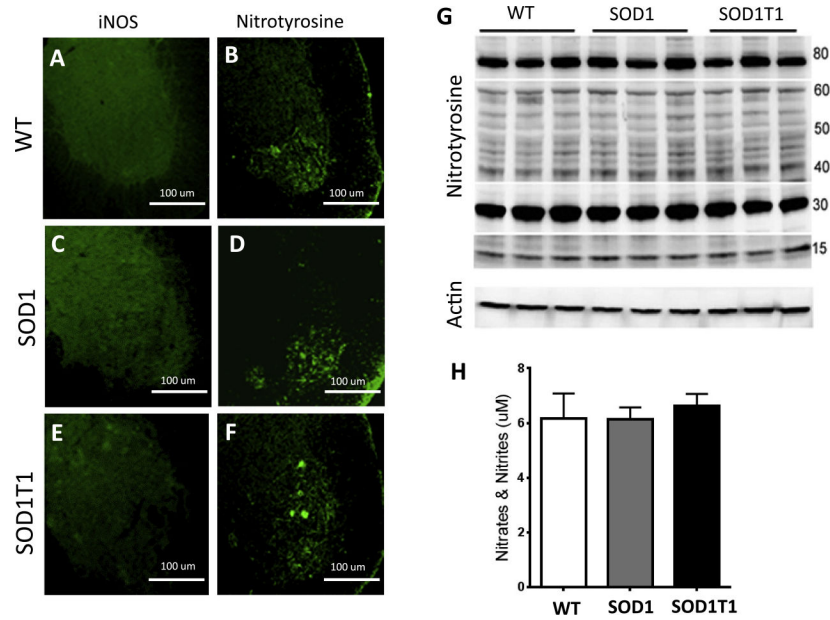
mice compared to controls there is no difference between the SOD1 and SOD1 T1mice (F). Histograms showing the quantification of western blots of TNF-R1 (G) and VEGF (H) in E, F. n.s.; not significant. * p < 0.05.

Fig. 5.

The Nitric oxide signaling pathway in SOD1 mutant mice is not affected by TrkB.T1 deletion at 12 weeks of age. (A-F) iNOS and Nitrotyrosine immunofluorescence images of lumbar spinal cords from WT (A, B), SOD1 (C, D) and SOD1-TrkB.T1 KO (SOD1T1; E, F) mice. Note the lack of specific signal for iNOS immunoreactivity in all groups (A, C, E) while the nitrotyrosine immunofluorescence in the motoneuron region shows no difference between WT, SOD1 or SOD1T1 KO mice (B, D, F). (G) Western blot analysis of lumbar spinal cords isolated from WT, SOD1 and SOD1T1 KO mice showing unchanged nitrosylation levels of proteins between 15 and 80 kDa. (H) Histogram showing the levels of nitrites and nitrates in lumbar spinal cords by colorimetric analysis. N = 5 animals/genotype.
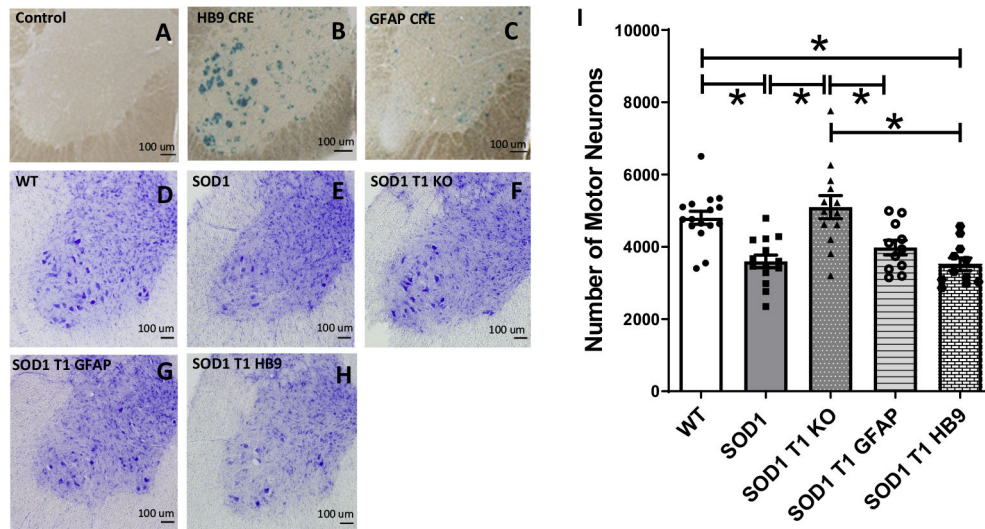
Fig. 6.

Deletion of TrkB.T1 in motoneurons or astrocytes of SOD1 mutant mice does not rescue motoneuron death at 12 weeks of age. (A-C) Representative β-Galactosidase staining images of lumbar spinal cords from a ROSA26-LacZ reporter mouse, used as negative control, (A), or a ROSA26-LacZ mouse crossed to a HB9-cre or a GFAP-cre transgenic showing specific cre activity in motor neurons (B) and astrocytes (C) respectively. (D—H) Representative Nissl staining of lumbar spinal cord sections of 12-week-old WT (D), SOD1 mutant (E), SOD1-TrkB.T1 KO (F), and SOD1 mice with an astrocytes (G; SOD1 T1 GFAP) or motoneuron-specific (H; SOD1 T1 HB9) TrkB.T1 knockout. (I) Histogram showing quantification of motor neuron numbers in the different mouse groups. Note that contrary to the SOD1 mutants with complete TrkB.T1 knockout showing rescue of motoneurons at 12 weeks, SOD1 mutants with specific TrkB.T1 deletion in either motoneurons or astrocytes are indistinguishable from SOD1 transgenic mice. Analysis of data was done by ANOVA followed by post-hoc Tukey's multiple comparison test. * indicates $p < 0.05$. $N = 11$–16/ group (WT, $n = 16$; SOD1, $n = 14$; SOD1 T1, $n = 12$; SOD1T1 GFAP, $n = 11$; SOD1T1 HB9, n = 11).
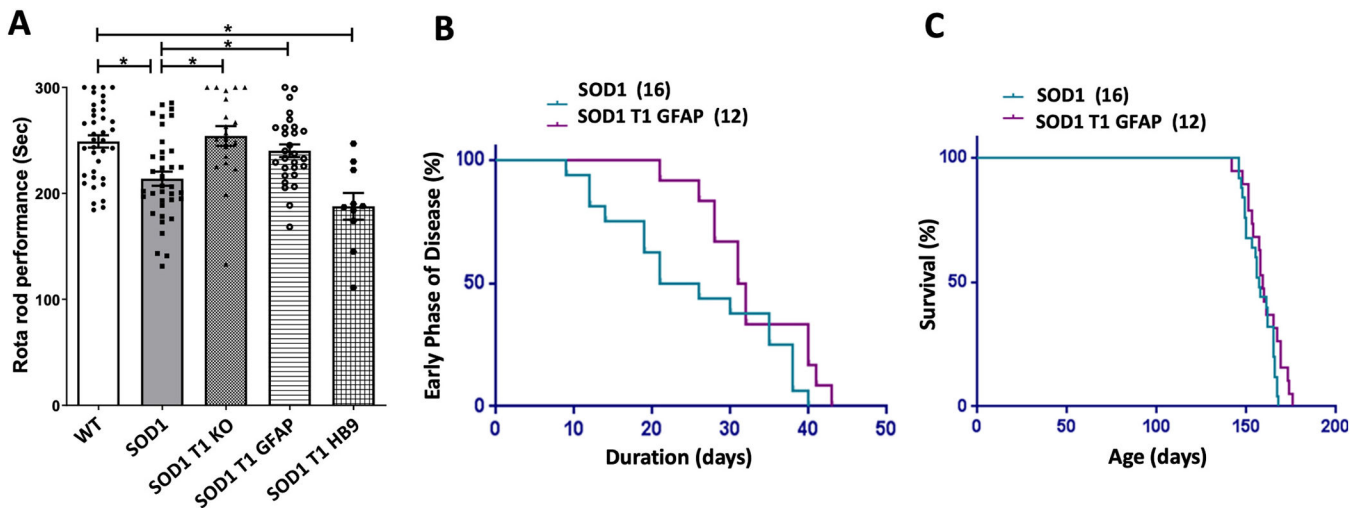
Fig. 7.
Muscle weakness and progression of disease after deletion of TrkB.T1 in SOD1 mutant mice. (A) Histogram showing rota-rod performance of animals of the indicated genotypes at 12 weeks of age. Animals were evaluated for muscle strength and co-ordination on the accelerating rota-rod test. Note that both global (SOD1 T1 KO) as well as astrocyte-specific deletion of TrkB.T1 in the SOD1 background (SOD1 T1 GFAP) improves rota-rod performance while motor neuron specific deletion (SOD1 T1 HB9) does not provide any protection. Analysis of data was done by ANOVA followed by post-hoc Dunn's multiple comparison test. * $p < 0.05$, $n = 37$ WT, 37 SOD1, 20 SOD1-T1, 28 SOD1-T1 GFAP and 10 SOD1-T1 HB9. (B, C) Diagrams showing the Kaplan-Meier curve of the duration of the early phase of disease (B) and survival (C) of SOD1 transgenic mice compared with SOD1 mice with astrocyte specific deletion of TrkB.T1. The number of animals for each group is indicated in parentheses.